Transmission electron microscopy of experimentally deformed hornblende

D. J. Morrison-Smith

Department of Earth and Space Sciences, State University of New York
Stony Brook, New York 11794

Abstract

Specimens of hornblende single crystals, deformed by Rooney *et al.* (1973, 1974), have been investigated by TEM. The main deformation features appear to be ($\bar{1}01$) twins, frequently containing high densities of dislocations. The major slip system appears to be (100) [001], with minor contributions from (010) [001], (010) [100], and (001) [100] also being possible. The strain contributed by the latter dislocations appears, however, to constitute only a small fraction of the strain accommodated by each specimen. A possible mechanism for the twinning process is constructed by considering the available observations in terms of details of the crystal structure. In addition the abundance of the various deformation mechanisms is discussed on the basis of crystallographic constraints.

A significant amount of sub-microscopic exsolution is observed in all specimens, frequently as small (100) and ($\bar{1}01$) lamellae, while in deformed regions a form of exsolution consisting of (100) platelets aligned along dislocations is observed. This mode of exsolution is considered to have occurred during the experiments, and a mechanism is proposed which involves preferential nucleation of the second phase in the local stress field of the dislocations.

Introduction

An extensive series of deformation experiments has recently been performed by Rooney, Riecker and co-workers (1970, 1973, 1974, 1975) in order to elucidate the deformational properties of amphiboles. These experiments were performed in a solid-pressure-medium apparatus at confining pressures from 5 to 20 kbar and temperatures from 27 to 1200°C at strain rates of 10^{-4} to 10^{-6} sec^{-1} using both single crystal and polycrystalline specimens of hornblende and tremolite.

Stress-strain curves obtained from these experiments indicate that amphiboles are exceedingly strong, although they sometimes exhibit weakening phenomena at high temperatures (>800°C) and high pressure (>15 kbar). Optical microscopy indicates that in single crystals twinning on ($\bar{1}01$) (using the $C2/m$ space group for hornblende) appears to be the major deformation mechanism at temperatures up to 600°C in specimens deformed parallel to [001]. In specimens of other orientations, slip along {110} cleavage planes appears to accommodate most of the strain. In specimens deformed above 800°C no deformation twins were observed for any orientation.

In polycrystalline specimens, plastic strain may be accommodated by deformation of the minor biotite components, twinning on ($\bar{1}01$), or kinking. The orientation of kinking is consistent with slip on the system (100) [001].

In specimens deformed at temperatures of 1000°C or greater, there was some deformation and melting of the amphiboles in the hotter parts of the specimens. Also, a large number of lamellar features were observed in these specimens, satisfying the criteria proposed by Carter (1965) for deformation lamellae in quartz; it was not possible, however, to define the nature of these features from optical microscopy.

This paper extends the work of Rooney and co-workers, presenting the results of an electron microscope study of several of the specimens deformed by them (Rooney *et al.*, 1973, 1974). These were single crystal samples from both the Canadian and Bamle hornblendes, compressed parallel to [001], at temperatures up to 600°C and at a strain rate of 10^{-5}sec^{-1}. In addition, several undeformed samples of these materials were observed in order to compare microstructures before and after deformation.

Experimental details

Standard petrographic thin sections were cut from each specimen and mounted with low melting point

resin onto glass slides. During optical observation small brass rings were glued around interesting areas, after which the specimens were separated from the glass slides by heating and trimmed with a scalpel blade to fit into a Commonwealth Scientific ion thinner (Heuer *et al.*, 1971), which was operated at 7–8 kV using argon ions. After thinning, samples were carbon coated to prevent charge build up during observation in the electron microscope. Observations were undertaken using a Philips EM300 electron microscope operating at 100 kV, utilizing a double tilt stage producing rotations of ± 30° about two mutually perpendicular axes.

Results

In the undeformed material there are only a few dislocations, averaging $\sim 10^6$ cm^{-2}, which may be the result of growth processes or may have been introduced during previous natural deformation events. Many of these dislocations are found as parts of small subgrain walls (Fig. 1) whose component dislocations may either be straight and parallel or take the form of hexagonal networks. The remaining dislocations appear to be randomly distributed through the specimen, generally straight but with a variety of orientations.

The only other feature observed in undeformed specimens is a low density of small coherent exsolution lamellae parallel to both (100) and ($\bar{1}$01). They are generally less than 5 μm long and 1000Å thick with smaller cell dimensions than the surrounding matrix. These observations are considered in more detail below in comparison with exsolution features observed in deformed specimens.

The most striking features of the optical studies of deformed hornblendes were twins lying parallel to ($\bar{1}$01); these features are also prominent in the specimens investigated here. The width of these twins varies from $\sim$ 1μm to $\sim$0.1 mm, the frequency of occurrence being approximately inversely proportional to their width. On the electron microscope scale the twins appear simply as slabs of material of different orientation to the host, bounded by flat, planar boundaries (Fig. 2). Diffraction patterns taken of both the twin and host appear to be related by a 180° rotation about [$\bar{1}$01]*. This is the normal to the twin boundary, and this relationship is consistent with that obtained by Rooney *et al.* (1970, 1973). The boundaries of the twins appear to be completely coherent with no dislocation structures or strain ap-
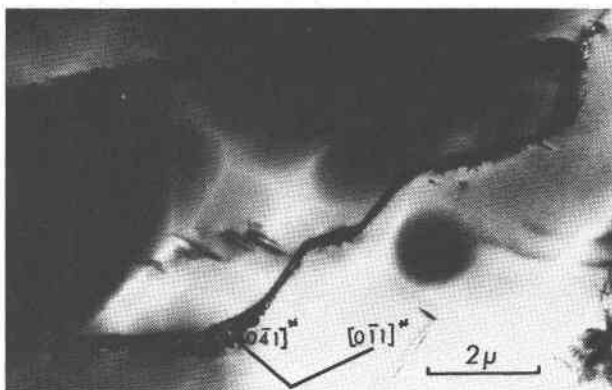

FIG. 1. A small subgrain of hornblende, shaped like an upside-down shoe, is outlined by a black border that consists of concentrations of those dislocations that are typical of undeformed specimens. The vast majority of these dislocations are parallel to [100], which is perpendicular to the page. The directions of reciprocal lattice vectors [0$\bar{4}$1] and [0$\bar{1}$1] are as shown.

parently associated with the interface. There have been no observations of growth features in these twins; even the narrowest are of great lateral extent and the termination of a twin within the specimen has not yet been observed.

The most noticeable feature in many of these twins is a high density of dislocations, usually lying on (100) planes of the twin, although there have been several observations of dislocations on other planes. The individual dislocation segments are so arranged that they appear to be segments of concentric loops apparently emanating from some central source such as a Frank-Read source (see Fig. 5 and 6 of Rooney *et al.*, 1975). In the smaller twins there appears to be an extremely high density of dislocations emanating from each source. The density in these small (less than 5μ thick) twins is frequently higher than 10^{10} cm^{-2}. This density, however, decreases markedly with increasing width.

Attempts to calculate the Burgers vectors of the observed dislocations were hampered by: (a) lack of sections of all orientations—all sections had been cut such that they lay between (130) and ($\bar{1}$30) and it was not possible to obtain reflections with diffraction vectors close to (010); and (b) difficulty in obtaining strict 2 beam cases and complete invisibility of dislocations.

For the case of dislocations lying in (100) arrays, invisibility was obtained for $g = 400$ and a marked reduction in contrast was obtained for $g = 130$, strongly suggesting that Burgers vector $b = [001]$. Assuming the plane of the arrays represents the slip plane, these observations are compatible with the
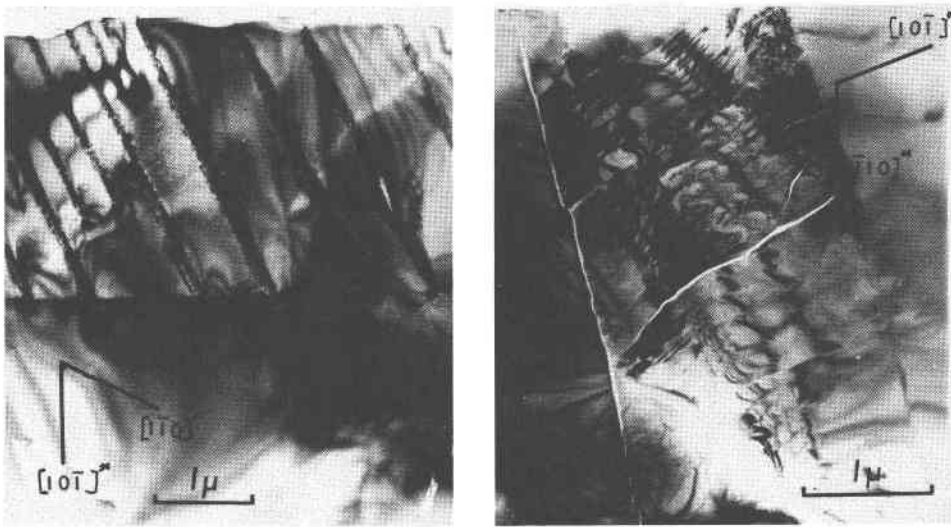
FIG. 2. Examples of ($\bar{1}01$) deformation twins in experimentally deformed hornblende: (a) shows the boundary parallel to ($\bar{1}01$) between a larger ($\sim 10\mu$ wide) twin (top) and the matrix (bottom); note the planar boundary containing no dislocations and the arrays of dislocations lying on (100) within the twin; (b) a small twin (N-S central section) showing a higher density of dislocation arrays than the larger twin in (a); one of the twin boundaries is defined by a crack that was probably formed subsequent to the twinning.

optical measurements made by Rooney and Riecker (1973).

There have been occasional observations of dislocation arrays on (010) and (001), the former being more common. They appear to be lying in their slip planes, but there have been insufficient observations of these dislocations to perform reliable Burgers vector determinations. Using the available specimens, dislocations in (001) arrays and in some (010) arrays can be put out of contrast using $g = 002$, but no other invisibility conditions were obtained. This suggests that $b = [100]$ is possible in both systems, but that $b = [001]$ may also be found in (010) arrays.

In some areas that have been strained only slightly, such as in the cooler ends of specimens (Carter and Avé Lallement, 1970, discuss temperature distributions within specimens in a Griggs-type solid-pressure-medium apparatus), deformation twins are observed that contain no dislocations, regardless of the size of the twin.

In untwinned material, the density of dislocations is very low in all specimens so far investigated, the average density being 10^6–10^7 cm^{-2}. The density is highest in specimens taken to higher overall strains, but the total amount of plastic deformation attributable to dislocation motion in the host material appears to be small in all cases.

Exsolution lamellae, parallel to both (100) and ($\bar{1}01$), are observed in most specimens (Fig. 3). Gen-

erally they exhibit different contrast from the matrix and offsets in extinction contours typical of exsolution lamellae in other amphiboles (Gittos et al. 1974) and pyroxenes (Boland, 1972; Champness and Lorimer, 1973). These exsolution lamellae appear to be coherent with the host, no misfit dislocations having been observed. In addition there do not appear to be any dislocations associated with growth ledges or steps as observed by Gittos et al. (1974). The surfaces of the lamellae, however, do not appear to lie precisely parallel to crystallographic planes; not only do they taper smoothly to their ends, but they are sometimes observed to be slightly curved or to bend round each other (e.g., Fig. 3b). It has not been possible to undertake direct lattice imaging with the present electron microscope due to a vibration problem in the building in which it is housed. Thus it was not possible to duplicate the investigation of unit-cell-height ledges observed in pyroxenes (Champness and Lorimer, 1974; Van der Sande and Kohlstedt, 1974) which could produce the observed curvature.

Electron diffraction patterns taken so as to include both host and lamella exhibit marked spot-splitting, indicating that the material in the lamella has a smaller unit cell than the host. The major changes in cell dimensions are for the crystallographic axes normal to the lamella, while there are only small differences in the axes that are parallel to the lamella boundary.
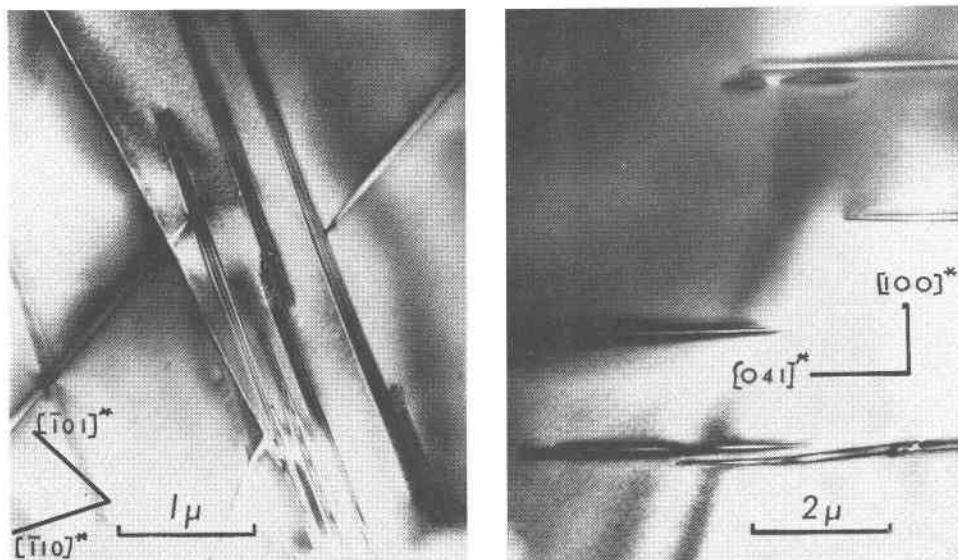
FIG. 3. Exsolution lamellae in experimentally deformed hornblende. (a) (100) lamellae trending approximately N-S are inclined slightly to the foil normal. The ($\bar{1}$01) lamellae trend approximately NE-SW. There is a V-shaped crack also running across the field of view. (b) (100) lamellae lying perpendicular to the foil showing smoothly tapered outlines and a slight bend where two lamellae bypass each other. There do not appear to be any dislocations associated with the boundaries of these lamellae.

In undeformed specimens lamellae are generally 0.5–5 μm long and up to 1000Å thick, whereas in many areas of the deformed specimens there is a significant number of lamellae approximately 20–30 μm long and 0.2–0.3 μm thick plus a comparable density of smaller lamellae, $\lesssim$ 5 μm long and ~1000Å thick. In some areas the density of lamellae becomes comparatively high (*e.g.* Fig. 3a).

Some additional exsolution features are observed only in deformed specimens (Morrison-Smith, 1974). Structures typical of this form of exsolution are illustrated in Figure 4. They generally consist of platelets from 0.2 to 1.0 μm in diameter lying parallel to (100) and aligned approximately parallel to [001]. In cross section (Fig. 5) the platelets can be seen to be discus-shaped with a maximum thickness of 500–1000Å. Furthermore these platelets are found *en echelon* at an angle of 10–20° to the (100) plane. Electron diffraction measurements indicate that the material within the platelets has a similar unit cell size to the previously described (100) exsolution lamellae, suggesting that they are of similar composition. Figure 4 shows the platelets exhibiting concentric extinction fringes which are acting as effective thickness contours. The compositional differences between the two phases result in slightly different scattering factors, and this leads to a difference in the extinction distance in the two phases. For each point on the surface

of the foil, the apparent thickness due to the presence of a platelet of different composition is given by

$$\Delta t = \xi_1 x \left(\frac{1}{\xi_1} - \frac{1}{\xi_2} \right)$$

where ξ_1 and ξ_2 are the extinction distances in the host and lamella respectively and x is the thickness of the lamella parallel to the electron beam at the point under consideration (Hirsch *et al*, 1965).

A sharp discontinuity is frequently observed in the fringe patterns, being more readily visible in the regions of overlap between platelets, running parallel to the axis of the array but displaced to one side (Fig. 4b). Under suitable diffracting conditions, this discontinuity can be associated with a dislocation running through the platelets. It can be seen more easily in the cooler regions of specimens where the platelets tend to be smaller and more widely spaced (Fig. 6).

In the more highly deformed regions of many specimens, bands of sheared, fractured, and rotated material (Fig. 7) give evidence for brittle failure. These features generally take the form of lamellar slabs that have been produced by shear parallel to their major faces, the strain being accommodated by fracture and parting of the material within the bands. The slabs vary in width from ~0.1 to 4 μm wide and frequently lie parallel to (100) and (001) planes, although they are not restricted to low index crystallographic
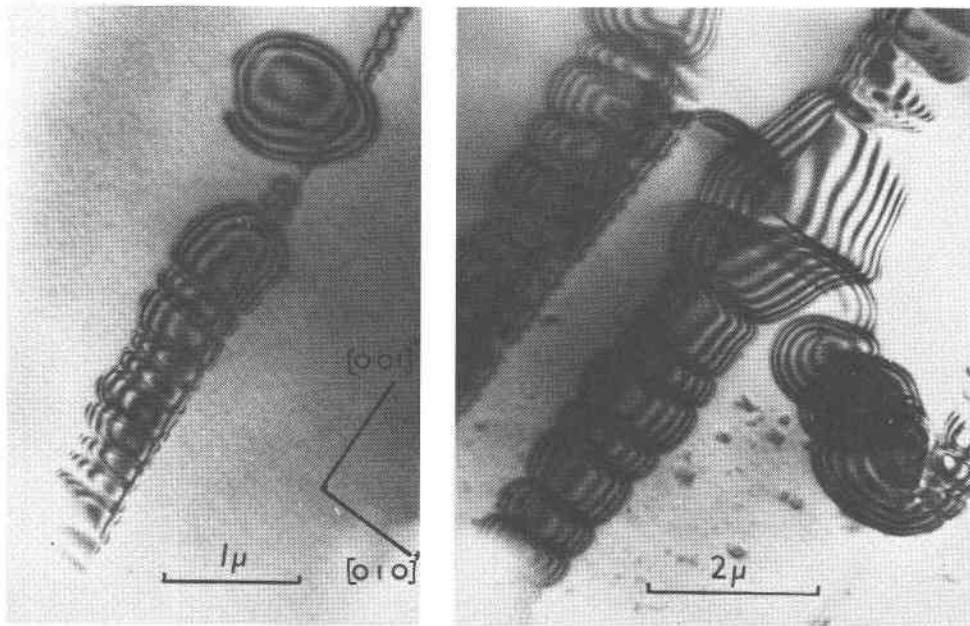
FIG. 4. (100) exsolution platelets observed in deformed specimens. The concentric extinction fringes are effective thickness contours and the contrast due to a dislocation running through each array can be clearly seen. (a) shows rather uncommon rapid changes in platelet diameter along the array. (b) shows a high density of arrays with additional platelets trending away from the dislocations.

planes. The narrower of these features appear similar in many ways to the objects associated with optical deformation lamellae in some experimentally deformed quartz (Christie and Ardell, 1974), although the features observed in these experiments have no associated dislocations such as were found by Christie and Ardell. There have been no optical observations of deformation lamellae in specimens deformed at temperatures less then 600°C (Rooney and Riecker, 1973). Thus it is not yet possible to correlate these features on the basis of available observations.

Discussion

The observations described in the previous section indicate that plastic deformation by the propagation of dislocations is not the major deformation mechanism in hornblende, and that deformation twinning accounts for an appreciable proportion of the strain. Consideration of the crystal structure of hornblende as compared to other silicates may give some insight into this behavior.

Dislocations

The energy to create a dislocation is proportional to the square of its Burgers vector (Nabarro, 1967); thus the preferred slip systems will involve slip parallel to the shortest lattice vectors, which for hornblende are [001] = 5.299Å and [100] = 9.885Å. [010] Burgers vectors would have energies approximately
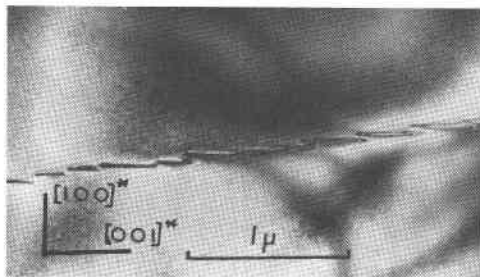

FIG. 5. Section through an array of platelets showing the approximate discus shape and *en echelon* arrangement of the platelets, running at ~ 10° to (100).
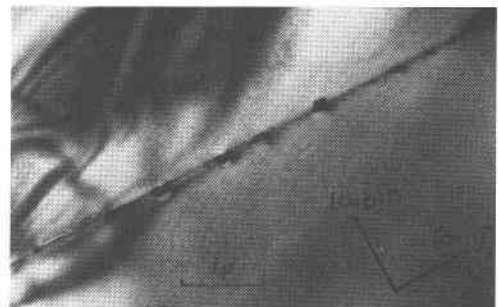

FIG. 6. Dislocation showing small precipitates nucleated along its length. Note that the precipitates are formed preferentially on one side of the dislocation line.

ten times higher than [001] and are, therefore, extremely unlikely. The quoted cell dimensions are taken from the work of Rooney *et al.* (1970).

Slip of dislocations involves breaking atomic bonds across the slip plane in which they are moving; hence the energy to move a dislocation depends on the density and nature of the bonds broken. The (100) plane is parallel to the double chains of tetrahedra and the sheets of octahedra, so that slip on this plane involves breaking metal–oxygen bonds between these layers. The (010) and (001) planes, however, cut through the layers of polyhedra such that the bond densities across these planes are higher than across (100). Hence slip would appear to be easier parallel to (100).

The deductions of the preceding paragraphs indicate that slip in hornblende should occur predominantly on the system (100) [001], with possible contributions from (010) [100]. These remarks are in general agreement with the observed slip systems, in that the majority of the dislocations appear to be on the system (100) [001] with occasional slip on (010) and (001).

These considerations give some indication of the relative magnitudes of the critical resolved shear stresses for the various slip systems. For compression in any given direction, however, the relationship between the actual resolved shear stress and the critical stress of each system will decide which of them operates initially. For instance, in this series of experiments there is no resolved shear stress on the system (100) [001] in the matrix crystal for compression parallel to [001], while in the twinned regions it frequently appears to exceed the critical stress, resulting in the generation of high densities of dislocations. These high densities are due in part to low dislocation mobilities but mainly to the fact that the resolved shear stress in the matrix on (100) [001] is negligible. Thus dislocations reaching the boundary will not be able to continue into the matrix and so produce a pile-up. In order to maintain the imposed strain rate a large number of dislocations must be generated by the available sources within the twin. The enhanced stress at the head of the pile-up, due to the dislocations within it, may eventually become high enough that the leading dislocations can be punched through into the matrix (Nabarro, 1967), as has been observed in several specimens.

($\bar{1}01$) Deformation twins

It appears unlikely that twinning on ($\bar{1}01$) can be produced by the passage of a series of partial disloca-
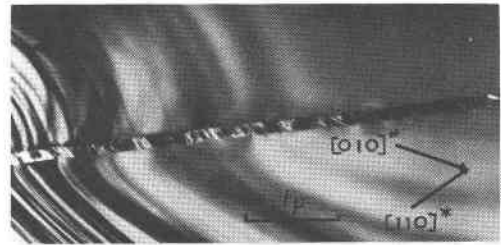

FIG. 7. Lamella of sheared material lying parallel to (110) consisting of blocks of fractures and rotated material.

tions as normally found in the case of metals (Sleeswyk, 1974). This mechanism generally involves the interaction of a moving partial dislocation with a stationary screw dislocation which is approximately perpendicular to the slip plane of the partial dislocation. Interaction of these dislocations converts the slip plane of the partial into a spiral around the screw, which may expand under the influence of an applied stress to produce a lamella of material transformed to the twin orientation. In order to twin the more complex mineral structures, however, the chains, layers, and polyhedra must be rotated within the unit cells.

To produce the observed morphology of ($\bar{1}01$) twins the above pole mechanism and subsequent reorientation of polyhedra would appear to require a high energy due to the amount of bond breaking involved. It would also appear that the great extent of the ($\bar{1}01$) twins would require extremely high dislocation velocities to propagate the twins in the duration of the experiment. It would appear that dislocation propagation at such high velocity in this plane is unlikely as this is a higher energy slip system than has been observed to operate in hornblende. There have been no observations of slip on ($\bar{1}01$) in these experiments.

A simpler method involving a martensitic type transformation (Petty, 1970) is described below. In the case of ($\bar{1}01$) twins in hornblende the twinning is seen simplistically as a shear of the unit cell parallel to ($\bar{1}01$), the (100) planes being rotated through approximately 30°. In detail it appears that the bulk of the transformation can be achieved by shear, and this seems to require negligible diffusion although some M–O bonds are broken. Using the cell dimensions and twin parameters given by Rooney *et al* (1970) for this hornblende, the twin relation can be constructed most simply by a shear parallel to (100) such that the tetrahedral chains are simply rotated about their vertices as shown in Figures 8 and 9, where the pivot points (P_1, P_2 . . . P_i) all lie in ($\bar{1}01$). All the tetra-
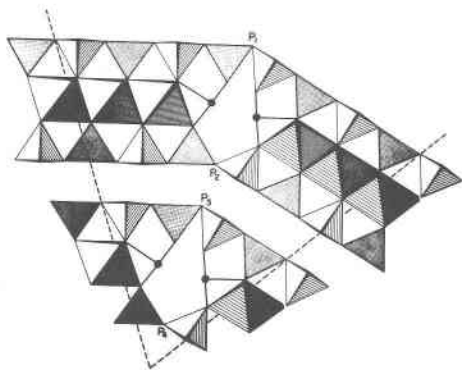
FIG. 8. Schematic (010) section of the twinned hornblende structure showing the proposed arrangement of tetrahedra and octahedra that correspond to the observed twin relations and cell dimensions. The points P_I are common to both twinned and untwinned structures and lie in ($\bar{1}01$).

hedra are rotated in the same sense (clockwise in this projection) which results in a shearing of the octahedral layer, with the upper layers of oxygen atoms (O_D–O_F in Fig. 9) being displaced with respect to the lower layer (O_I–O_K). Viewed from within the octahedral layer, this can be seen as a rotation of the oxygens about the cations M_C and M_D. The movement is such that bonds like M_D–O_D are broken as O_D rotates about M_C while new bonds such as M_D–O_I are formed as O_I is rotated towards M_D (the M_B–O_I bond having been broken). Similarly, M_D–O_K bonds are

broken and M_D–O_F formed in order to complete the formation of new octahedra in the twinned orientation.

In the twin boundary the bonding of tetrahedra is continuous while the octahedral bonding is disrupted across the interface. For example, in the untwinned state (Fig. 9a) M_C is bonded to O_C while in the fully twinned orientation it would be bonded to O_H. In the case (Fig. 9b) where it lies close to the boundary it is not clear to which oxygen it will be bonded across the interface. It is possible that it does not retain any bonds across the interface and that electrostatic repulsion from M_B leads to some sort of five-coordinated site, with M_C displaced towards O_E.

Available evidence indicates that the critical resolved shear stress for twinning is between 2 and 4 kbar (Rooney et al., 1973, 1974). This is apparently lower than the critical shear stress for dislocation motion on this plane, as there have been no observations of dislocations on ($\bar{1}01$). The magnitude of this stress suggests, however, that the transformation is controlled by some form of dislocation motion. The most likely slip plane appears to be (100), although there have been no observations of dislocations that could be associated with the twinning process. All observed dislocations on (100) appear to be introduced subsequent to the twinning.

Exsolution

Electron diffraction patterns have shown that the cell dimensions in exsolution lamellae are smaller than the surrounding material; however, these measurements are not sufficiently accurate to define the composition of the second phase. Such measurements cannot be made using X-ray diffraction because the amount of exsolved material ($\lesssim$ 0.1% vol.) is below the detection limits of present techniques. However, published data (e.g., Papike et al., 1969; and Ross et al., 1969) indicate that the relative cell dimensions are compatible with (100) lamellae being composed of cummingtonite in a hornblende matrix. In addition the increased extinction distance observed in the lamellae as compared to the host indicates a smaller scattering factor than the matrix (cf. Boland, 1972) which could be due to Mg enrichment and/or Ca depletion within the lamellae: this is also consistent with the lamellae being composed of cummingtonite.

The cell dimensions for the ($\bar{1}01$) lamellae, however, do not appear to correspond to any common amphiboles. It is possible that the material in the ($\bar{1}01$) lamellae has anomalous cell dimensions due to
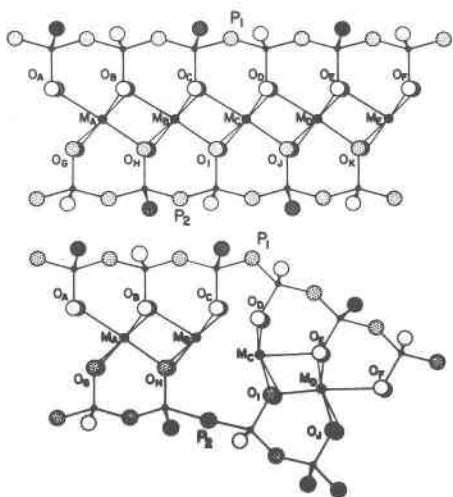

FIG. 9. (010) sections through a single tetrahedral-octahedral-tetrahedral layer, indicating the bond rearrangements required by a martensitic-type transformation to produce the twin arrangement shown in Figure 8. (a) shows the untwinned situation while in (b) part of the layer has been twinned with respect to the original orientation. Similarly labelled ions are equivalent in (a) and (b) and the details of bond rearrangements are discussed in the text.

the constraining effect of the surrounding host material (see Morimoto and Tokonami's work on pyroxenes, 1969, and Smith's work on perthites, 1961). The composition of these particular lamellae is, therefore, unclear.

It would appear that there is extensive development of (100) exsolution during the experiments in this particular hornblende. Most of this exsolution takes the form of (100) platelets as shown in Figure 4. It is well documented in the metallurgical literature that dislocations frequently act as sources for precipitation in alloys and that this precipitation can be dramatically enhanced by an applied shear stress (see recent review by Nicholson, 1970). It may be that a similar process is active in this case, as a dislocation appears to be associated with each array of platelets (Figs. 4, 6). Surrounding any edge dislocation are regions of compression and dilation due to the "extra half plane" as visualized in any simplistic model of an edge dislocation (Fig. 10a). Nucleation of a unit cell of precipitate involves elastic distortions in both phases if the cell dimensions are different and the associated elastic energy constitutes part of the energy barrier to nucleation of the second phase. If, however, the precipitate can nucleate in a region where the host is already distorted, as in the local stress field of a dislocation where the elastic energy involved in nucleation is reduced, then this region will become a site of preferred nucleation. As indicated earlier, the unit cell of the precipitate happens to be smaller than that of the host, so that nucleation should take place preferentially in the compressive region of the stress field of the dislocation.

As the precipitate grows, interfacial energy considerations become important and govern the subsequent precipitate morphology. As the major differences in cell dimensions between the two phases are in the *a* dimension, an interface parallel to (100) will have a significantly lower elastic misfit energy associated with it than any other crystallographic plane; thus the development of large (100) surfaces should be preferred (Fig. 10c). Inhomogeneous nucleation along a dislocation line inclined at a small angle to (100) should lead to the development of *en echelon* arrays of platelets (Fig. 10d), precisely as has been observed in these experiments. Inhomogeneous nucleation is apparently not uncommon in alloys (Nicholson, 1970) although the nuclei are not usually as widely spaced as appears to be the case in these observations. The reason for these widely spaced nuclei is not clear, but it does allow the platelets to grow to large size before interacting. This mechanism of
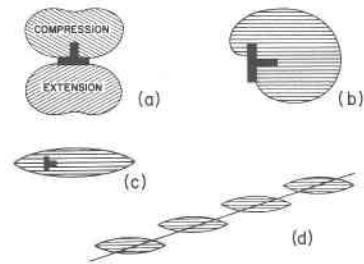

FIG. 10. (a) Simple representation of an edge dislocation. The vertical bar represents the "extra half plane" and the horizontal bar is parallel to the trace of the slip plane and the Burgers vector. The regions of compression and extension around the dislocation are indicated. (b) Precipitates with a smaller unit cell than the host would be nucleated preferentially in the compressive stress field of the dislocation. When the precipitate has outgrown the effects of the local stress field it may spill over to the other side of the dislocation. (c) During subsequent growth, elastic misfit energies govern precipitate morphology. The misfit is minimal across (100) so that platelet surfaces develop parallel to this plane. (d) Inhomogeneous nucleation of precipitates along a dislocation inclined at a small angle to the platelet's surface leads to the development of *en echelon* arrays as observed by TEM.

precipitation appears to explain all the observed features of these platelets.

Conclusion

This preliminary series of investigations of experimentally deformed hornblendes has shown that the predominant features of this type of deformation consist of $(\bar{1}01)$ deformation twins with a lesser contribution from dislocations. The proposed twinning mechanism consists essentially of a martensitic-type shear in which very little diffusional motion of atoms is required, whereas one third of the M–O bonds in octahedra are broken and remade as new octahedra are assembled in the twin orientation. The tetrahedra are simply rotated about their vertices.

The predominant slip system in these experiments appears to be (100) [001], which is explicable in terms of [001] being the shortest possible Burgers vector and (100) slip planes requiring the lowest density of broken bonds, implying that this system has the lowest dislocation energy and lowest critical resolved shear stress. Similar considerations indicate that (010) [001], (010) [100], and (001) [100] are also possible slip systems. The observations, however, were not able to establish definitely that these systems are operative, although there is evidence to indicate that they have occurred in these experiments.

A significant amount of exsolution is seen in these specimens, and there is good evidence to show that

exsolution is occurring during the experiments. This exsolution takes the form of (100) platelets arranged along a dislocation, and it appears that the second phase is being precipitated preferentially in the local stress field of the dislocation. Such a mode of exsolution could be enhanced by a suitably directed stress.

Acknowledgments

References

BOLAND, J. N. (1972) Electron petrography of exsolution in an enstatite-rich orthopyroxene. *Contrib. Mineral. Petrol.* **37,** 229–234.

CARTER, N. L. (1965) Basal quartz deformation lamellae—A criterion for recognition of impactites. *Am. J. Sci.* **263,** 786–806.

———, AND H. G. AVE LALLEMENT (1970) High-temperature flow of dunite and peridotite. *Geol. Soc. Am. Bull.* **81,** 2181–2202.

CHAMPNESS, P. E., AND G. W. LORIMER (1973) Precipitation (exsolution) in an orthopyroxene. *J. Mater. Sci.* **8,** 467–474.

———, AND ——— (1974) A direct lattice resolution study of precipitation (exsolution) in orthopyroxene. *Phil. Mag.* **30,** 357–365.

CHRISTIE, J. M., AND A. J. ARDELL (1974) Substructure of deformation lamellae in quartz. *Geology,* **2,** 405–408.

GITTOS, M. F., G. W. LORIMER, AND P. E. CHAMPNESS (1974) An electron-microscopic study of precipitation (exsolution) in an amphibole (the hornblende-grunerite system). *J. Mater. Sci.* **9,** 184–192.

HEUER, A. H., R. F. FIRESTONE, J. D. SNOW, H. W. GREEN, R. G. HOWE, AND J. M. CHRISTIE (1971) An improved ion-thinning apparatus. *Rev. Sci. Instrum.* **42,** 1177–1184.

HIRSCH, P. B., A. HOWIE, R. B. NICHOLSON, D. W. PASHLEY, AND M. J. WHELAN (1965) *Electron Microscopy of Thin Crystals.* London, Butterworths, 549 p.

MORIMOTO, N., AND M. TOKONAMI (1969) Oriented exsolution of augite in pigeonite. *Am. Mineral.* **54,** 1101–1117.

MORRISON-SMITH, D. J. (1974) A mechanism of exsolution in amphiboles (abstr.). *Geol. Soc. Am. Abstr. Programs,* **6,** 878.

NABARRO, F. R. N. (1967) *Theory of Crystal Dislocations.* Oxford, 821 p.

NICHOLSON, R. B. (1970) *Nucleation at Imperfections in Phase Transformations.* Am. Soc. for Metals, Ohio, p. 269–309.

PAPIKE, J. J., M. ROSS, AND J. R. CLARK (1969) Crystal-chemical characterization of clinoamphiboles based on five new structure refinements. *Mineral. Soc. Am. Spec. Pap.* **2,** 117–136.

PETTY, E. R., Editor (1970) *Martensite; Fundamentals and Technology.* London, Longmans, 205 p.

ROONEY, T. P., AND R. E. RIECKER (1973) Constant strain rate deformation of amphibole minerals. *Air Force Cambridge Res. Lab. Env. Res. Pap.* **430,** 33 p.

———, ———, AND M. ROSS (1970) Deformation twins in hornblende. *Science,* **169,** 173–175.

———, A. T. GAVASCI, AND R. E. RIECKER (1974) Mechanical twinning in experimentally and naturally deformed hornblende. *Air Force Cambridge Res. Lab. Env. Res. Pap.* **484,** 21 p.

———, R. E. RIECKER, AND A. T. GAVASCI (1975) Hornblende deformation features. *Geology,* **3,** 364–368.

ROSS, M., J. J. PAPIKE, AND K. W. SHAW (1969) Exsolution textures in amphiboles as indicators of subsolidus thermal histories. *Mineral. Soc. Am. Spec. Pap.* **2,** 275–299.

SLEESWYK, A. W. (1974) Perfect dislocation pole models for twinning in the f.c.c. and b.c.c. lattices. *Phil. Mag.* **29,** 407–421.

SMITH, J. V. (1961) Explanation of strain and orientation effects in perthites. *Am. Mineral.* **46,** 1489–1493.

VAN DER SANDE, J. B., AND D. L. KOHLSTEDT (1974) A high resolution electron microscopy study of exsolution lamellae in enstatite. *Phil. Mag.* **29,** 1041–1049.